PHYSICAL REVIEW B **88**, 060502(R) (2013)

Strong- versus weak-coupling paradigms for cuprate superconductivity

Shahaf Asban,[1] Meni Shay,[1,2] Muntaser Naamneh,[1] Tal Kirzhner,[1] and Amit Keren[1,*]

[1]*Department of Physics, Technion–Israel Institute of Technology, Haifa 32000, Israel*

[2]*Department of Physics and Optical Engineering, Ort Braude College, P.O. Box 78, 21982 Karmiel, Israel*

(Received 28 May 2013; revised manuscript received 19 July 2013; published 2 August 2013)

Absolute resistivity measurements as a function of temperature from optimally doped $YBa_2Cu_3O_{7-\delta}$, $La_{2-x}Sr_xCuO_4$, $Bi_2Sr_2Ca_1Cu_2O_{8-x}$, and $(Ca_{0.1}La_{0.9})(Ba_{1.65}La_{0.35})Cu_3O_y$ thin films are reported. Special attention is given to the measurement geometrical factors and the resistivity slope between T_c and T^*. The results are compared with a strong-coupling theory for the resistivity derivative near T_c, which is based on hard core bosons, and with several weak-coupling theories, which are BCS based. Surprisingly, our results agree with both paradigms. The implications of these findings and the missing calculations needed to distinguish between the two paradigms are discussed.

DOI: 10.1103/PhysRevB.88.060502 PACS number(s): 74.25.Bt, 74.25.Gz, 74.25.Ha

Two major discoveries were made at a very early stage in the study of cuprate superconductivity. One was the Uemura relation for underdoped samples.[1] This relation states that $T_c \propto \lambda(0)^{-2}$, where T_c is the superconducting transition temperature, and $\lambda(0)$ is the magnetic penetration depth at zero temperature. This relation was found using the muon spin rotation (μSR) technique. The second discovery was that for underdoping and optimal doping, at temperatures T above T^*, the resistivity $\rho_{\rm dc}(T)$ is a linear function of T.[2,3] Near optimal doping, T^* is similar to T_c and the linear relation extends down to T_c. Later on Homes extended the Uemura relation and showed that a broader scaling holds for both underdoped, optimally doped, and overdoped samples: $\rho_s(0) \propto \sigma(T_c)T_c$, where $\rho_s(0)$ is the superfluid density at zero temperature, and $\sigma(T_c) = 1/\rho_{\rm dc}(T_c)$ is the conductivity at T_c.[4] This observation was based on optical conductivity measurements. In many low doping models, $\rho_s(0) \propto \lambda^{-2}(0)$.[5] Therefore, the Homes law can be expressed as $\lambda^{-2}(0) \propto \sigma(T_c)T_c$. For both Homes' and Uemura's laws to coexist, $\sigma(T_c)$ must be universal for all underdoped cuprates.

Two kinds of theories address the Homes law. The first kind was provided by Tallon *et al.*,[6] and the latter by Imry, Strongin, and Homes,[7] and by Kogan.[8] They predict

$$\lambda(0)^{-2} = K\sigma(T_c)T_c, \tag{1}$$

where K ranges from 120, as in the original Homes law, to $K = 240$. These theories have a few elements in common. They assume weak coupling (WC), that the resistivity arises mainly from disorder, that the BCS relation between the superconducting gap and the critical temperature $\Delta \propto T_c$ is correct, and that the constant of proportionality (which varies a bit between authors) is on the order of unity. The big advantage of these theories is that they explain materials of all dopings. The disadvantage is that they treat a compound such as optimally doped $YBa_2Cu_3O_{7-\delta}$ (YBCO) as a dirty superconductor. In optimally doped YBCO, the resistivity extrapolates to zero at $T \to 0$ (see below), which can only occur in the absence of impurities. In fact, no experiment shows inhomogeneities in this compound.[9] In addition, the weak-coupling theories do not address the temperature dependence of $\sigma(T)$ for $T > T_c$, which is very different from simple metals.[10]

The second theory was provided by Lindner and Auerbach (LA).[11] They derived the relation $\rho_{\rm dc}(T) = 77.378(\frac{\lambda_{ab}(0)}{q})^2\frac{K_BT}{\hbar c^2}$ by using the hard core boson (HCB) model at half boson filling (optimal doping); $q = 2$ is the boson charge in units of e. The HCB model is expected to be valid for temperatures lower than T^*, where Cooper pairs are supposed to start forming in the cuprates. This theory assumes a clean system and that the resistivity arises from strong coupling (SC) between bosons. The LA derivation generates the Homes law for optimal doping; it also captures the linear resistivity and provides the coefficient of proportionality quantitatively. However, the theory is not valid for an underdoped or overdoped compound, which is a serious disadvantage. Due to impurities, the extrapolation to $T = 0$ of $\rho_{\rm dc}(T)$ is finite in some cuprates. Therefore, it is more practical to write the LA law in a differential form:

$$\frac{d\rho_{\rm dc}}{dT}(T > T_c) = 77.378\left(\frac{\lambda_{ab}(0)}{q}\right)^2\frac{K_B}{\hbar c^2}. \tag{2}$$

In this Rapid Communication, we check both the WC and SC theories, as accurately as possible, in the small region where both are valid, namely, optimal doping. We use direct current (dc) resistivity versus T measurements in films of $YBa_2Cu_3O_{7-\delta}$ (YBCO), $(Ca_{0.1}La_{0.9})(Ba_{1.65}La_{0.35})Cu_3O_y$ (CLBLCO), $La_{2-x}Sr_xCuO_4$ (LSCO), and $Bi_2Sr_2Ca_1Cu_2O_{8-x}$ (BSCCO). We take the geometrical factors of the film into account and check their influence experimentally. This allows us to determine $\rho_{\rm dc}(T)$ in absolute value, and to demonstrate that our results are indeed film-geometry independent. We then compare $\frac{d\rho_{\rm dc}}{dT}(T_c)$ to $\lambda^2_{ab}(0)$ and $\sigma(T_c)T_c$ to $\lambda^{-2}_{ab}(0)$, as in the SC and WC theories, respectively. λ_{ab} is taken from Refs. 12–15, respectively; the scatter in λ_{ab} values as provided by different authors is incorporated in the error bars as described below. Our main results, given in Fig. 1, are represented by the solid symbols. For comparison we also show $\frac{d\rho_{\rm dc}}{dT}(T > T_c)$ for single crystals of YBCO, LSCO, BSCCO, and $Tl_2Ba_2CuO_{6+\delta}$ (TBCO) taken from Refs. 2,16,17, respectively, versus λ^2_{ab} for single crystal taken from Refs. 6,14,18, respectively (open symbols).

In the case of the LA law, we fit our data to a straight line given by Eq. (2) with q as a fit parameter. We find $q = 1.75(15)$. The fit is shown in Fig. 1. We also depict in

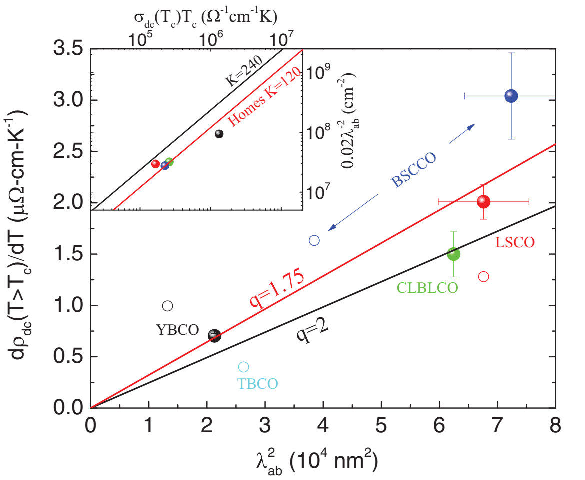

FIG. 1. (Color online) Solid symbols: The temperature derivative of the resistivity of four different optimally doped cuprate films, at $T > T_c$, obtained by dc measurements, as a function of their penetration depth. The solid lines show the best linear fit to the data (that extrapolates to the origin) and the prediction by the LA model. The values represented by open symbols are based on single crystal measurements. The inset shows a Homes-type law on a log-log scale generated from the same data. To get the same scales as Homes, we are forced to multiply λ^{-2} by 0.02. The original Homes observation, given by Eq. (1), with $K = 120$ and with the largest $K = 240$ obtained by WC predictions, are presented by solid lines.

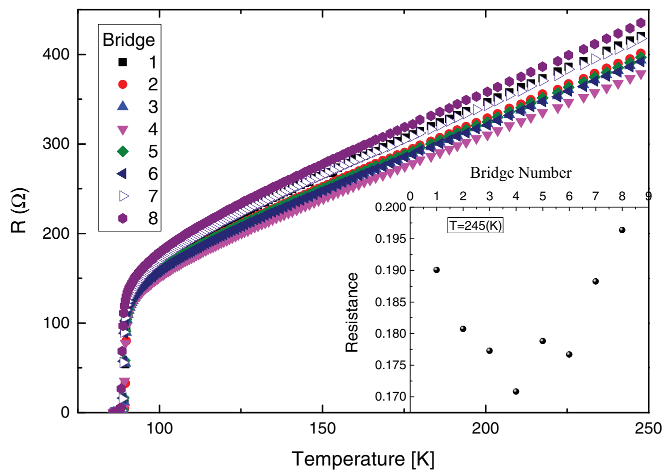

FIG. 2. (Color online) Measurements of resistance as a function of temperature in narrow bridges of optimally doped YBCO. Bridges 1 and 8 are close to the edges of the film. Bridges 3–6 are in the center of the film.

the figure the LA prediction with $q = 2$. The experimentally determined boson charge of $1.75(15)e$ is very similar to theoretical charge of $2e$. It means that the HCB model is self-consistent for the cuprates, and a very good starting point for understanding the conductivity of optimally doped samples. We also present our results as a Homes-type plot in the inset of Fig. 1. Since optical conductivity measures the plasma frequency which is proportional to $\lambda^{-2}(0)$, it leaves one free parameter. To achieve the same scales as Homes we multiply $\lambda_{ab}^{-2}(0)$ by 0.02. This 2% correction is due to the difference in the penetration depth and dc conductivity as estimated by optical conductivity measurements and the techniques used here.[19] With this scale we find that on a log-log plot our data are not far from Homes', which are represented by the solid line. We also show the WC theoretical predictions with $K = 240$ in Eq. (1).

It seems that both WC and SC theories are in agreement with our experiment. Another important piece of information is the indication of carriers with charge $2e$ around the superconducting-insulator transition. This indication comes from doping-temperature scaling relations of the resistivity.[20] The emerging picture is that the superconducting state in the cuprates is grainy, sometimes called Bose glass.[20] The SC HCB model is a good starting point for describing each grain. The normal metal between grains, in underdoped and possibly overdoped samples, plays an important role in determining the conductivity above the global T_c. This metal is best described by one of the WC theories. However, at optimal doping one grain takes over the entire sample. When this happens the conductivity is related only to the superconducting properties, as Eq. (2) predicts.

We now describe our experiment in more detail. A cardinal aspect of our measurement is the determination of the absolute value of the resistivity and resistivity derivative near T_c. One strategy is to use single crystals, but in this case one does not know exactly which route the current takes in the sample between contacts, and it is difficult to precisely determine the resistivity. Therefore, such measurements are usually done by preparing a film and patterning a bridge on it by ion milling. It is then assumed that the resistance is dominated by the bridge. However, in high temperature superconductors, close to T_c, the situation is not that simple. Figure 2 shows resistance measurements for a set of identical bridges. For this and other measurements, we used films grown on a 10×10 mm^2 $SrTiO_3$ (STO) substrate with the c axis perpendicular to the film. Due to flux flow resistance, the transition region from normal to the superconducting state is very rounded and it is difficult to determine $\frac{d\rho_{dc}}{dT}(T \gtrsim T_c)$. There is also variation in the resistance between different bridges. This variation is due to the film being less thick near the edges. The inset of Fig. 2 shows the resistance at $T = 245$ K as a function of bridge number. Indeed, the first and last bridges are more resistive, but the middle ones have very similar resistance. We therefore abandoned the bridge method, and focused on wide film measurements which sample the film center and have very sharp transitions, as shown in Fig. 3. However, in this case geometrical factors have to be taken into account when measuring resistivity.[21]

Our four-point probe measurement setup is shown in the inset of Fig. 3(b). The two external contacts are used as the current source and drain and the two internal contacts are the voltage probes. For a single current source at the origin in contact with a two-dimensional (2D) infinite conducting plane, the current density at a distance r from the source is given by $J = I/(2\pi r)$. The electric field on the conducting surface is set by $J = \sigma E$. This leads to a logarithmic potential $V - V_0 = -\frac{I}{2\pi}\rho_{dc} \ln r$. In a current source (a) and drain (b), with equal distance s between all probes, the potential difference is $\Delta V = \frac{I}{\pi}\rho_{dc} \ln 2$. For a finite sheet, the potential difference is found by introducing an infinite number of images to the original current

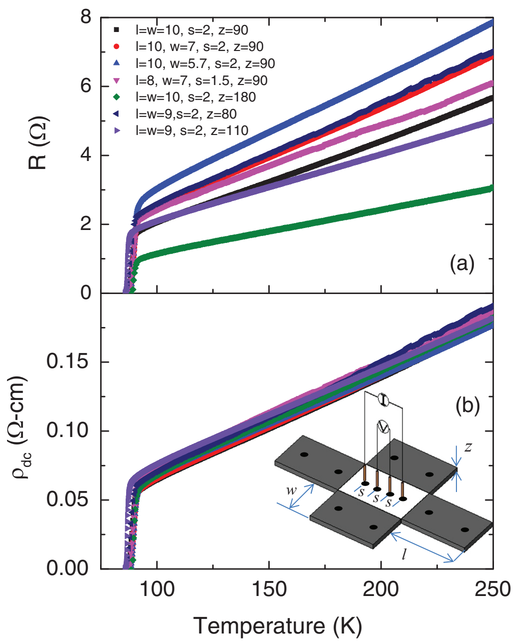

FIG. 3. (Color online) (a) Resistance vs temperature in films of different dimensions and different distances between contacts. (b) The resistivity obtained by using Eq. (4). The resistivity is geometry independent. The inset in (b) shows the experimental setup and the set of current images used to generate the correction factor calculated in Eq. (3).

source and drain, as shown by the spots on dark slabs in the inset of Fig. 3(b).[21] This forces the current to run parallel to the boundary. One then sums the potential from all images. The current sources and drains, and their images, are located on a lattice given by $r^a_{nm} = (mw, s + nl)$ and $r^b_{nm} = (mw, nl - 2s)$, where w and l are the width and length of the film, respectively. The potential difference between the two measured contacts is given by $\Delta V = \rho_{\mathrm{dc}} I C$, where

$$C = \frac{1}{2\pi} \sum_{n,m} (-1)^n \ln \left[\frac{(mw)^2 + (s + nl)^2}{(mw)^2 + (nl - 2s)^2} \right]. \quad (3)$$

C as a function of w for various l and a typical s is shown in Fig. 4. In our setup, C is on the order of 3.5. Therefore, it is

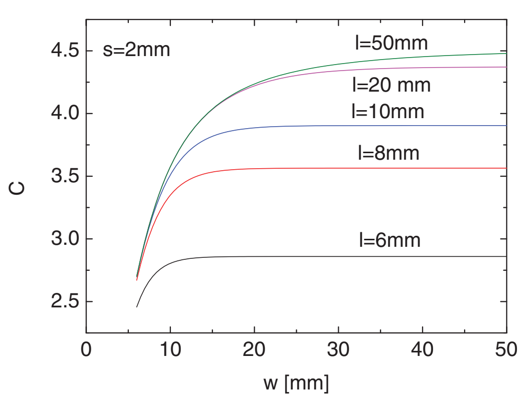

FIG. 4. (Color online) The geometrical factor C, calculated in Eq. (3), as a function of the width w for various lengths l, and a fixed distance between contacts s.

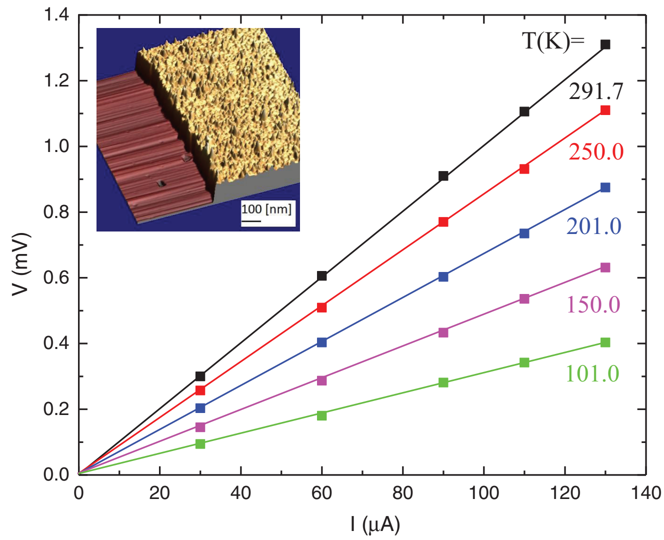

FIG. 5. (Color online) *V-I* measurements of the YBCO film at different temperatures, demonstrating the ohmic behavior of the film. The inset shows an AFM image of the film topography near an etched step.

essential to check that Eq. (3) is valid, as is done below. Another important factor is the film thickness z, which is measured by atomic force microscopy (AFM), as shown in the inset of Fig. 5. Each of the films was measured from all sides, and, unless stated otherwise, their thickness is 100 ± 5 nm. The resistivity is given by

$$\rho_{\mathrm{dc}} = \frac{1}{C} \frac{z \Delta V}{I}. \quad (4)$$

Current simulations show that only 7% of the total current passes close to the edges of the films where the resistance is high by 7% (see the inset of Fig. 2). This leads to an error of less than 1% on the resistivity due to the thickness measurement.

To check the validity of Eqs. (3) and (4), we produced YBCO films of various geometries and measured their resistance as presented in Fig. 3(a). The figure shows the resistance $(\Delta V/I)$ of seven different films with various heights z, widths w, lengths l, and distances between contacts s, in units of millimeters. Figure 3(b) depicts the resistivity ρ_{ab} obtained by Eq. (4). The resistivity is indeed geometry independent and linear immediately above T_c.

In Fig. 5, we show *V-I* measurements of one of the YBCO films. In the normal state, the films show ohmic behavior up to a current of 140 μA. Therefore, all our measurements are done in a current of 100 μA.

Finally, we present resistivity measurements in optimally doped films of YBCO, LSCO, BSCCO, and CLBLCO in Fig. 6. A pure linear behavior is observed only in YBCO, and, as expected, the resistivity extrapolates to zero at zero temperature. In LSCO, the substrate reduces T_c from the bulk value considerably, due to a mismatch in lattice parameters. This lattice mismatch also reduces the T_c of the other compounds, but not as much as in LSCO. To simplify our analysis, we focus on the temperature range 100–200 K, which, for all materials, is higher than T_c, higher than the region of fluctuating superconductivity, and lower than T^*. In this temperature range, the reduction of T_c in LSCO is not

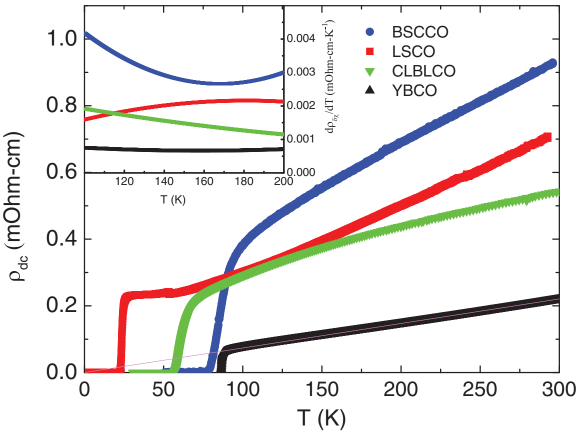

FIG. 6. (Color online) Resistivity vs temperature for four different optimally doped cuprates. The inset shows the temperature derivative between 100 and 200 K, which is above T_c and below T^* for all materials. The average derivative is used in Fig. 1. The solid line demonstrates that, for YBCO, $\rho_{dc}(T \to 0) = 0$.

relevant. In the inset of Fig. 6, we present the first derivative of the resistivity as a function of temperature. As expected, the derivative is a constant only for YBCO. For the other materials, the derivative varies slowly with temperature. We treat the derivative as a statistical variable and assign to each material an averaged resistivity slope and standard deviation over the entire plotted range. The standard deviation is used to generate the error bars. The summary of our thermal derivative of the resistivity versus magnetic penetration depth results is plotted in Fig. 1. As mentioned before, the penetration depth is taken from the literature. For optimally doped YBCO film, $\lambda_{ab} = 146 \pm 3$ nm was determined in a theory-free method using slow muons.[12] In this case, the value of λ_{ab} agrees with coated sample resonance (CSR) measurements, which is also a theory-free method,[15] and the error bar is known. For YBCO crystal, $\lambda_{ab} = 115 \pm 3$ was also measured with slow muons.[18] For LSCO, there are only crystal measurements and all values reported are scattered around 260 ± 15 nm.[14] For BSCCO, the $\lambda_{ab} = 270 \pm 15$ nm value was taken from CSR with its error bar.[15] For BSCCO and TBCO crystals the values of $\lambda_{ab} = 196$ and $\lambda_{ab} = 162$, respectively, are from Ref. 6. They have been measured by a few techniques but no error bar is assigned. Finally, CLBLCO was measured only by standard μSR, where the determination of $\lambda_{ab} = 250$ nm involves theoretical arguments and the error bar is not known.[13]

A comparison between our experimental results and both WC and SC theories show that both are valid for optimally doped samples to some extent. To distinguish between the two, the WC theories should be extended to provide $\sigma(T > T_c)$. Similarly, the SC theory should be broadened to include the doping dependence of $\rho(T > T_c)$. We believe that there is room for a third theoretical approach that combines the two paradigms into one, in order to account for the full doping and temperature variations. As for optimal doping, the fact that the resistivity above T_c is determined by a superconducting quantity only is an amazing property of the cuprates.

We would like to thank Gad Koren for the use of his film preparation laboratory. In addition, we are grateful for helpful discussions with N. H. Lindner, A. Auerbach, and Y. Imry. This research was funded by the Israeli Science Foundation.

*keren@physics.technion.ac.il

[1] Y. J. Uemura *et al.*, Phys. Rev. Lett. **62**, 2317 (1989).
[2] Y. Ando, S. Komiya, K. Segawa, S. Ono, and Y. Kurita, Phys. Rev. Lett. **93**, 267001 (2004).
[3] N. Barišić, M. K. Chan, Y. Li, G. Yu, X. Zhao, M. Dressel, A. Smontara, and M. Greven, Proc. Natl. Acad. Sci. USA **110**, 12235 (2013).
[4] C. C. Homes, S. V. Dordevic, T. Valla, and M. Strongin, Phys. Rev. B **72**, 134517 (2005).
[5] K. Bernardet, G. G. Batrouni, J.-L. Meunier, G. Schmid, M. Troyer, and A. Dorneich, Phys. Rev. B **65**, 104519 (2002).
[6] J. L. Tallon, J. R. Cooper, S. H. Naqib, and J. W. Loram, Phys. Rev. B **73**, 180504 (2006).
[7] Y. Imry, M. Strongin, and C. C. Homes, Phys. Rev. Lett. **109**, 067003 (2012).
[8] V. G. Kogan, arXiv:1305.3487.
[9] R. Ofer, S. Levy, A. Kanigel, and A. Keren, Phys. Rev. B **73**, 012503 (2006).
[10] J. C. Garland and R. Bowers, Phys. Rev. Lett. **21**, 1007 (1968).
[11] N. H. Lindner and A. Auerbach, Phys. Rev. B **81**, 054512 (2010).
[12] T. J. Jackson, T. M. Riseman, E. M. Forgan, H. Glückler, T. Prokscha, E. Morenzoni, M. Pleines, Ch. Niedermayer, G. Schatz, H. Luetkens, and J. Litterst, Phys. Rev. Lett. **84**, 4958 (2000).
[13] A. Keren, A. Kanigel, J. S. Lord, and A. Amato, Solid State Commun. **126**, 39 (2003).
[14] Q. Li, M. Suenaga, T. Kimura, and K. Kishio, Phys. Rev. B **47**, 2854 (1993); C. Panagopoulos, B. D. Rainford, J. R. Cooper, W. Lo, J. L. Tallon, J. W. Loram, J. Betouras, Y. S. Wang, and C. W. Chu, *ibid.* **60**, 14617 (1999); F. Gao, D. B. Romero, D. B. Tanner, J. Talvacchio, and M. G. Forrester, *ibid.* **47**, 1036 (1993).
[15] R. Prozorov, R. W. Giannetta, A. Carrington, P. Fournier, R. L. Greene, P. Guptasarma, D. G. Hinks, and A. R. Banks, Appl. Phys. Lett. **77**, 4202 (2000).
[16] T. Watanabe, T. Fujii, and A. Matsuda, Phys. Rev. Lett. **79**, 2113 (1997).
[17] A. Carrington, A. P. Mackenzie, D. C. Sinclair, and J. R. Cooper, Phys. Rev. B **49**, 13243 (1994).
[18] R. F. Kiefl, M. D. Hossain, B. M. Wojek, S. R. Dunsiger, G. D. Morris, T. Prokscha, Z. Salman, J. Baglo, D. A. Bonn, R. Liang, W. N. Hardy, A. Suter, and E. Morenzoni, Phys. Rev. B **81**, 180502(R) (2010).
[19] S. V. Dordevic, D. N. Basov, and C. C. Homes, Nat. Sci. Rep. **3**, 1713 (2013).
[20] A. T. Bollinger, G. Dubuis, J. Yoon, D. Pavuna, J. Misewich, and I. Božović, Nature (London) **472**, 458 (2011).
[21] F. M. Smits, Bell Syst. Tech. J. **34**, 711 (1958).